

## Article

# Biomechanical Behavior of Different Miniplate Designs for Skeletal Anchorage in the Anterior Open Bite Treatment

Ana Paula Macarani Ielpo<sup>1</sup>, Jefferson David Melo de Matos<sup>1,2</sup> , Pedro Yoshito Noritomi<sup>3</sup>,  
Guilherme da Rocha Scalzer Lopes<sup>1</sup> , Daher Antonio Queiroz<sup>4,\*</sup> , Alexandre Luiz Souto Borges<sup>1</sup>   
and Rodrigo Dias Nascimento<sup>1</sup>

- <sup>1</sup> Department of Biomaterials, Dental Materials, and Prosthodontics, Institute of Science and Technology, São Paulo State University (Unesp), São José dos Campos 05508-070, SP, Brazil  
<sup>2</sup> Department of Restorative Dental Sciences, Center for Dental Biomaterials, University of Florida (UFHealth), Gainesville, FL 32611, USA  
<sup>3</sup> Renato Archer Information Technology Center, Campinas 13069-901, SP, Brazil  
<sup>4</sup> Department of Restorative Dentistry & Prosthodontics, School of Dentistry, The University of Texas Health Science Center Houston (UTHealth), Houston, TX 77054, USA  
\* Correspondence: daher.antonio.queiroz@uth.tmc.edu

**Abstract:** This study aimed to evaluate the stress distribution and mechanical behavior of miniplate designs to skeletal anchorage for the treatment of anterior open bite in adult patients. A complete hemimaxilla, teeth, brackets, transpalatal bar, and three miniplates were virtually modeled. I-, Y-, and T-shaped miniplates were installed in the area of the alveolar zygomatic crest. The assembly was constricted and three intrusive forces (2, 4, and 6 N) were applied to the maxillary molars and anchorage according to the miniplates. All materials were considered homogeneous, elastic, and linear; the mesh was 1,800,000 hexahedrons with 2,800,000 nodes on average. Displacement, maximum principal stress, and von Mises stress were evaluated according to the shape of the anchorage device and intrusive force. The miniplate configurations resulted in different stress and displacement intensities in the bone tissue and plate; these stresses were always located in the same regions and were within physiological limits. The Y-plate showed the best performance since its application generated less stress in bone tissue with less displacement.

**Keywords:** orthodontic anchorage; miniplates; anterior open bite



**Citation:** Ielpo, A.P.M.; de Matos, J.D.M.; Noritomi, P.Y.; da Rocha Scalzer Lopes, G.; Queiroz, D.A.; Borges, A.L.S.; Nascimento, R.D. Biomechanical Behavior of Different Miniplate Designs for Skeletal Anchorage in the Anterior Open Bite Treatment. *Coatings* **2022**, *12*, 1898. <https://doi.org/10.3390/coatings12121898>

Academic Editors: Egemen Avcu, Mert Guney and Yasemin Yildiran Avcu

Received: 1 November 2022

Accepted: 2 December 2022

Published: 5 December 2022

**Publisher's Note:** MDPI stays neutral with regard to jurisdictional claims in published maps and institutional affiliations.



**Copyright:** © 2022 by the authors. Licensee MDPI, Basel, Switzerland. This article is an open access article distributed under the terms and conditions of the Creative Commons Attribution (CC BY) license (<https://creativecommons.org/licenses/by/4.0/>).

## 1. Introduction

Anterior open bite (AOB) has a multifactorial etiology and can be divided into dental or skeletal open bites. The diagnosis of the type of open bite is essential for correct treatment [1].

Providing adequate anchorage is necessary for the treatment of malocclusion. In the case of severe AOB, orthognathic surgery is one of the therapeutic options. However, in addition to its higher risks and costs, and the fact that it can only be performed after the end of the growth cycle, this procedure encounters resistance from some patients. In some non-surgical cases, the intrusion of the maxillary molars with the aid of skeletal anchorage should be performed. This approach permits to balance of existing morphological differences and improves facial esthetics [2]. Skeletal anchorage devices such as mini-implants, miniplates, and osseointegrated implants have been widely used in these situations [3–5]. Previous studies have evaluated mandibular molar intrusion using miniplates in the cortical bone, more precisely in the areas of the apex of the first and second molars, and reported intrusion movement of 3 to 5 mm without major changes in the occlusal plane. Using a fixed miniplate anchorage, the magnitude of the force can be better controlled, thus reducing root resorption by lowering the forces applied [6,7]. In this sense, the present study evaluated the biomechanical behavior of different anchorage plates, since the use of

these devices makes the treatment very safe in terms of the risk of root resorption in the apex of the intruded tooth.

Treatment with miniplates is advantageous since it does not require preparation at the site of installation, the device is screw-retained in the patient's bone, and the only necessary preparation is the individualization of the miniplate according to the anatomy of the alveolar zygomatic crest [6–8]. The T, Y, and I shape are more easily molded to the maxilla, while L-shaped miniplates better fit the jaw [8].

Finite element analysis (FEA) can be used to model the structures of artificial and natural tissues permitting the application of forces in the most diverse directions. Furthermore, it is possible to obtain information about the level of stress at the chosen site, whether a tooth or tissue, caused by the applied load [9]. Since it is a numerical analysis, the FEA can measure the force, stress, strain, and deflection of miniplates, thus predicting any possibility of clinical failure by excessive load. In addition, this method permits the evaluation of the bone stress resulting from the shape of the anchorage device and the number of screws necessary for the fixation of the plate [10].

This study aimed to evaluate the stress distribution and behavior of different miniplate designs by finite element analysis based on the experienced stresses and displacement, simulating a clinical situation of skeletal anchorage for the treatment of AOB in an adult patient.

## 2. Materials and Methods

Three types of orthodontic miniplates (I, Y, and T shapes) were evaluated to determine which shape would cause less bone stress and would exhibit the best mechanical behavior after the application of intrusion forces of 2, 4, and 6 N to the maxillary posterior teeth for the treatment of AOB in an adult patient. The project and analysis were conducted in collaboration with the Renato Archer Information Technology Center (Campinas, São Paulo, Brazil).

### 2.1. Elaboration of the Model

The industrial design of the three-dimensional (3D) images of the titanium miniplates was created with the SolidWorks software (SolidWorks Corporation, Concord, MA, USA) based on the measurements of commercially available plates (Figure 1).

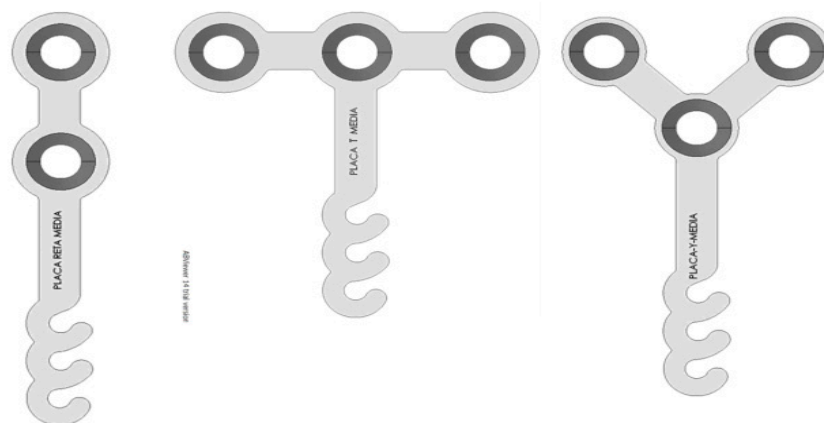


**Figure 1.** I-, T-, and Y-shaped miniplates.

The 3D finite element model was created with the Rhinoceros 4.0 software (SR 9.0, McNeel, Seattle, WA, USA) from a maxilla with 1 mm cortical bone available in the database of the Institute of Science and Technology, Unesp, São José dos Campos [11,12]. In this software, each type of plate was positioned in the alveolar zygomatic crest of the maxilla. The three types of plates had the same pattern of juxtaposition contact with the bone tissue. The fixation screws and plates were made of commercially pure titanium and were

fabricated in the model with sliding contact to more closely resemble clinical reality [13]. The plates were modeled virtually to allow perfect adaptation and reduction of the bone-plate interface. Each miniplate was first positioned in the 3D model in the area of the alveolar zygomatic crest so that another fold could be subsequently introduced in the active part of the plate to arrange it parallel to the long axis of the tooth (Figure 2).

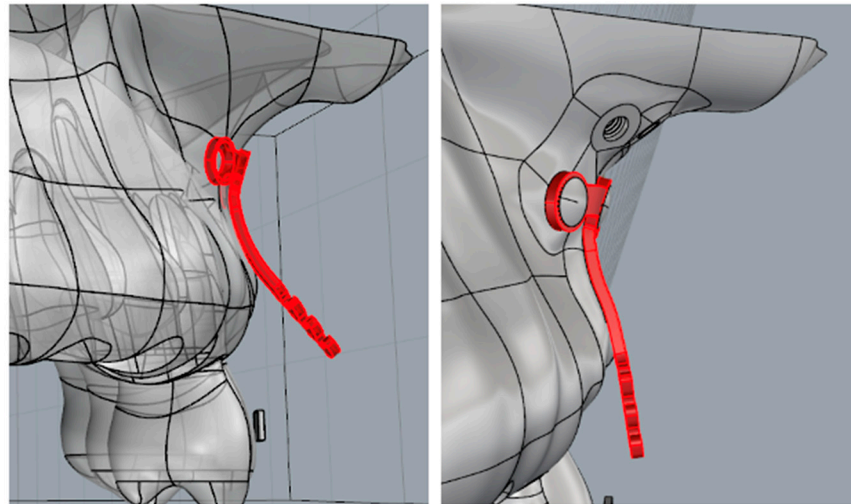


**Figure 2.** Position of the miniplate in the model.

An adult maxilla was considered in the model, with conventional Roth Light Slot 22 orthodontic brackets (Morelli, Sorocaba, SP, Brazil) being fixed to the teeth and bands to the maxillary molars with hooks [14]. All devices were anchored with rectangular orthodontic Nitinol wire (0.017 × 0.025) [12]. The entire set of orthodontic devices remained anchored in the transpalatal bar to prevent buccal movement of the maxillary first molar when the intrusion was performed. The transpalatal bar was placed at an ideal distance to the mucosal space and was attached to the accessory palatal tube in the maxillary first molars to achieve maximum absolute anchorage (Figure 3).

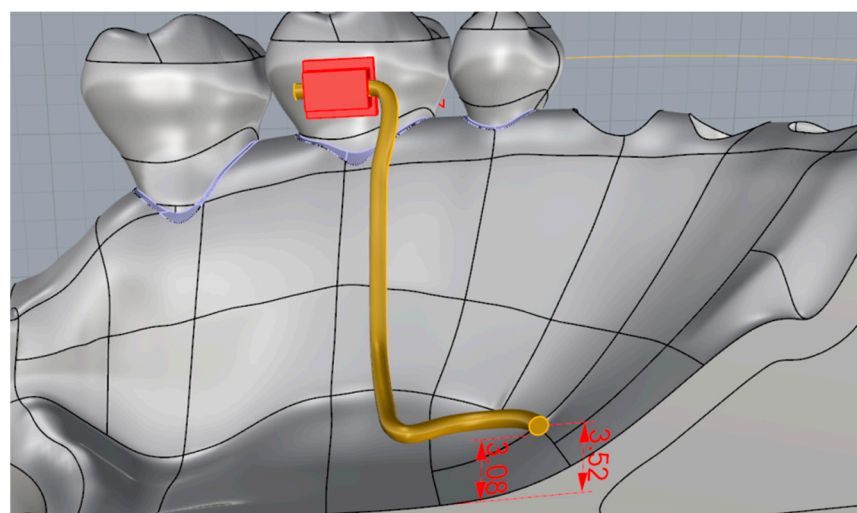


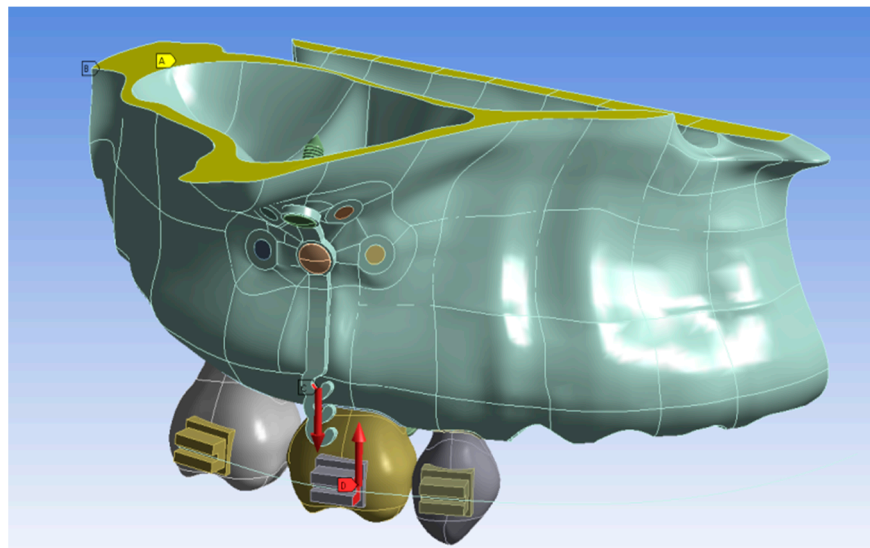
**Figure 3.** Position of the transpalatal bar in the model.

All materials were considered to be isotropic, linearly elastic, and homogeneous. The properties of the materials used in this study were obtained from the literature (Table 1) [15–21].

**Table 1.** Material properties used in the present numerical analysis.

Material	Young Modulus (GPa)	Poisson Ratio
Y-TZP [15]	220	0.30
Titanium [16]	110	0.30
Nitinol [18]	52	0.30
Stainless steel [19]	200	0.25
Cortical bone [20]	13.7	0.30
Cancellous bone [20]	1.37	0.30
Oral mucosa [21]	10	0.40
Periodontal ligament [21]	0.0118	0.45

Each miniplate was positioned in the virtual maxilla so that the hook to which the force would be applied was projected in the oral cavity at a distance of approximately 8 mm from the orthodontic arch. This approach permitted the generation of stress in the nickel–titanium elastic or spring coupled to the hook, as well as in the molar band tube, thus promoting posterior intrusion [22]. The intrusion force elastic was applied in the direction of the long axis of the tooth, always attached to the bracket and on the third hook of the miniplate, corresponding to the ideal distance (Figure 4).

**Figure 4.** The direction of force application for posterior intrusion.

## 2.2. Pre-Processing

The produced 3D models were transferred to the analysis software (17.2 ANSYS Inc., Houston, Tx, USA) (Figure 5) [11]. During this phase, axial forces of 2, 4, and 6 N were applied, simulating posterior intrusion and consequent treatment of open bite [23]. Now it was possible to generate the mesh of finite elements for the different regions and to attribute different material properties (Table 1). The number of nodes and elements generated is described in Table 2.

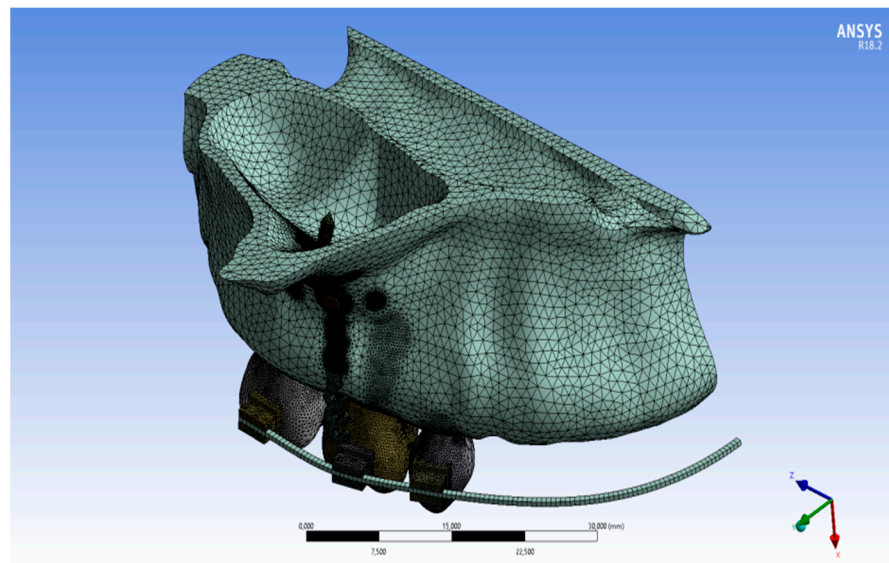


**Figure 5.** Mesh generated from the three-dimensional model.

**Table 2.** Material properties used in the present numerical analysis.

	Number of Nodes	Number of Elements
Plate I	2.900.228	1.923.115
Plate Y	2.847.272	1.891.437
Plate T	2.697.198	1.788.073

### 3. Results

The orthodontic miniplates and bone tissue were evaluated according to their biomechanical behavior within physiological limits. Results were obtained for nine simulations, three for each type of miniplate. Maximum principal stress (MPa), von Mises stress (MPa), and displacement (mm) were evaluated when the I, Y, and T plates were submitted to forces of 2, 4, and 6 N (Table 3).

**Table 3.** Displacement, maximum principal stress, and von Mises stress were obtained for three types of miniplates (I, Y, and T) submitted to loads of 2, 4, and 6 N.

Loads		2 N						4 N						6 N					
Miniplates	Displacement (mm)	Region	Maximum Principal Stress (MPa)	Region	Von Mises Stress (MPa)	Region	Displacement (mm)	Region	Maximum Principal Stress (MPa)	Region	Von Mises Stress (MPa)	Region	Displacement (mm)	Region	Maximum Principal Stress (MPa)	Region	Von Mises Stress (MPa)	Region	
I-plate	0.012	First hook of the plate	1.491	Border of inferior screw	41.699	Border of inferior screw and most superior hook	0.024	First hook of the plate	3.079	Border of inferior screw	83.397	Border of inferior screw and most superior hook	0.036	First hook of the plate	4.772	Border of superior screw	125.100	Border of inferior screw and most superior hook	
Y-plate	0.010	First hook of the plate	1.071	Border of inferior screw	44.076	Border of inferior screw and most superior hook	0.020	First hook of the plate	2.719	Border of inferior screw	88.152	Border of inferior screw and most superior hook	0.030	First hook of the plate	3.151	Border of right screw	132.230	Border of inferior screw and most superior hook	
T-plate	0.036	First hook of the plate	3.276	Border of central screw	65.346	Border of central screw and most superior hook	0.066	First hook of the plate	7.270	Border of central screw	139.950	Border of central screw and most superior hook	0.100	First hook of the plate	10.489	Border of central screw	193.060	Border of central screw and most superior hook	

Higher displacement was observed at the apex of the plate furthest from the screw, represented by the reddest area at the site where the elastic applies force to the tooth (Figure 6).

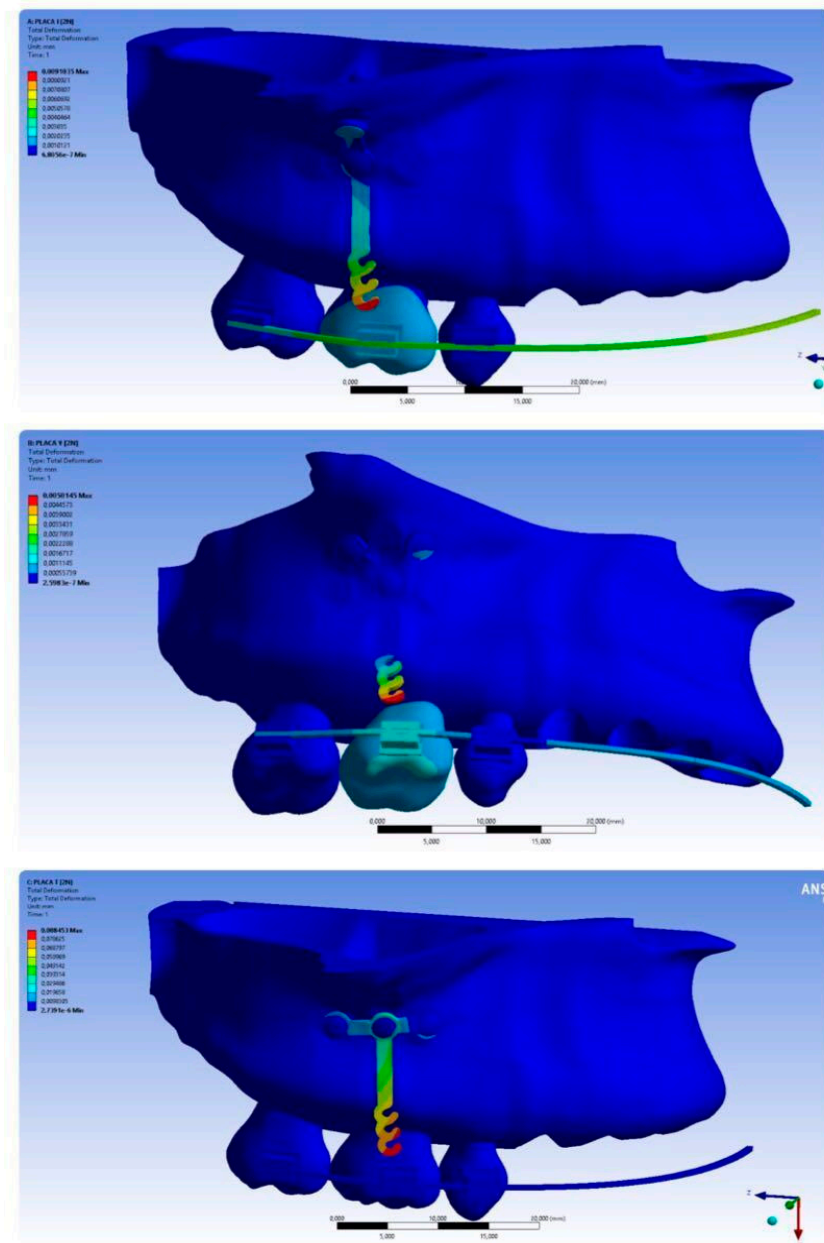
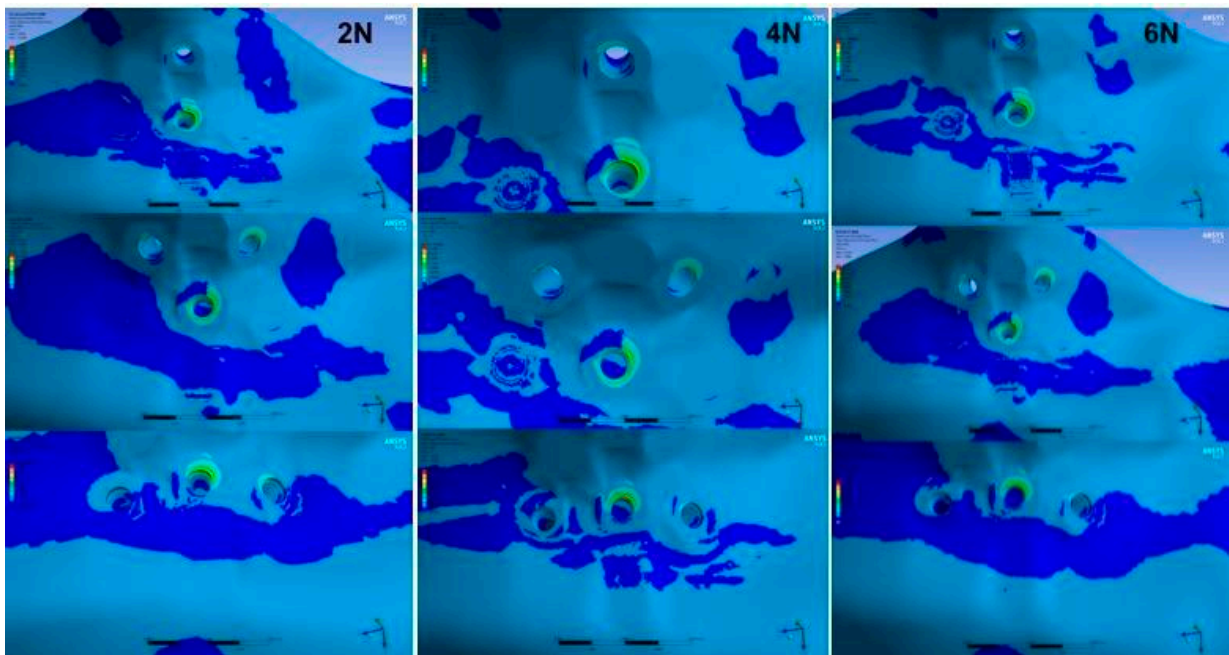


Figure 6. Mesh generated from the three-dimensional model.

The maximum principal stress was analyzed in bone tissue. Since the miniplate performs a movement in the inferior direction because of tension movement, the compression stress for the 2-N load was greater in the most inferior screw of the I-plate, as shown in Table 3. The maximum principal stress obtained for the 4-N load, i.e., stress caused in the bone tissue immediately after force application, originated at sites similar to the 2-N load, showing slightly higher intensities. For the 6-N load, the sites of greatest stress differed from the previous loads in models I and Y (Figure 7).



**Figure 7.** Mesh generated from the three-dimensional model.

The analysis of von Mises stress used for ductile solids demonstrated that the third hook region is the most requested in all miniplate models. In addition, there are some areas at the site of the screw where the plate suffers greater stress (Figure 8).

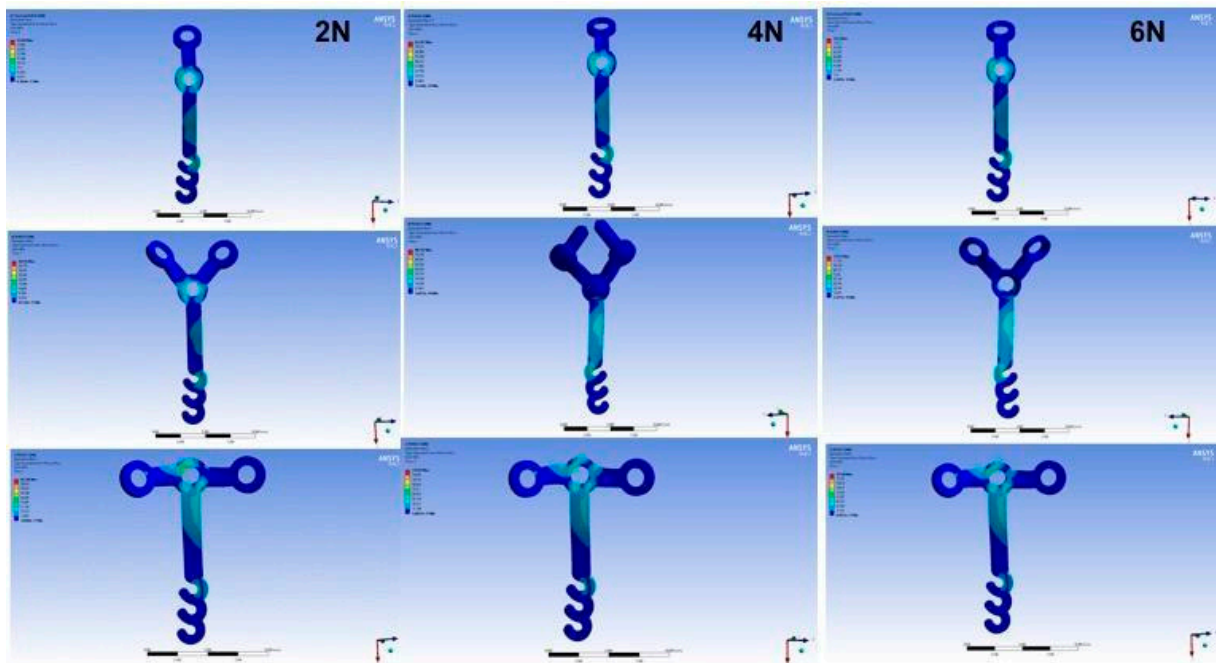


**Figure 8.** Maximum principal stress was obtained for each type of miniplate (I, Y, and T).

As can be seen, the displacement of each plate and the stress suffered by the miniplates and bone tissue increased exponentially proportionally to the load applied.

Considering the sample size limitation, statistical analysis was performed assuming a level of significance of 7% and a 95% confidence interval. Table 4 shows the data's descriptive statistics (mean  $\pm$  standard deviation). Comparison of the three miniplates

by ANOVA considering the three forces applied indicates that only displacement of the miniplates was within the level of significance ( $p < 0.07$ ).

**Table 4.** ANOVA for the results obtained: standard deviation; CI: confidence interval.

Group		Mean Value $\pm$ SD	N	CI	<i>p</i> -Value
Displacement	I-PLATE	0.024 $\pm$ 0.012	3	0.013	0.054
	T-PLATE	0.068 $\pm$ 0.032	3	0.036	
	Y-PLATE	0.020 $\pm$ 0.099	3	0.012	
Maximum principal stress	I-PLATE	3.114 $\pm$ 3.07	3	1.856	0.105
	T-PLATE	7.01 $\pm$ 3.6	3	4.088	
	Y-PLATE	2.31 $\pm$ 1.09	3	1.241	
Von Mises stress	I-PLATE	83.4 $\pm$ 41.7	3	47.19	0.488
	T-PLATE	131.45 $\pm$ 63.9	3	72.39	
	Y-PLATE	88.15 $\pm$ 44.08	3	49.88	

Thus, based on the mean values obtained in each test for the different forces, Tukey's multiple comparisons test was applied to determine which models the significant difference occurred (Table 5).

**Table 5.** Tukey's multiple comparisons test.

	Title	I-Plate	T-Plate
Displacement	T-plate	0.090	-
	Y-plate	0.972	0.068 *
Maximum principal stress	T-plate	0.191	-
	Y-plate	0.912	0.113
Von Mises stress	T-plate	0.518	-
	Y-plate	0.993	0.580

Legend: \* statistically significant difference ( $p < 0.07$ ).

The results showed that the difference in displacement was only statistically significant ( $p = 0.068$ ) when the T-plate (0.067275) was compared to the Y-plate (0.019996).

#### 4. Discussion

Treatment of AOB is complex because of the difficulty in correctly diagnosing etiological factors and in accurately determining the possible loss of vertical dimension in each patient [24]. Skeletal AOB is currently treatable with less invasive options and lower rates of morbidity by installing miniplates for the intrusion of maxillary and mandibular molars. This approach would be much more complex than conventional orthodontics, which requires the use of devices such as brackets, wires, and bands [6,25]. Miniplates are more efficient for posterior intrusion, a more stable process than prior extrusion, in addition to providing more favorable aesthetic and functional gains [25]. A nickel-titanium (nitinol) alloy wire was used to simulate a passive molar intrusion, as this wire is approximately 75% more flexible than a rigid splint [12,25,26]. In addition, this wire is presented as a memory alloy, allowing high fixed retentions. Therefore, due to the absence of high elasticities, possible plastic deformations are common. In this sense, it is suspected that unwanted tooth movements occur more rarely when compared to conventional orthodontic wires [26]. However, the present study has shown that the miniplate design can affect the mechanical response during orthodontic movement and its selection should be considered an important step during treatment planning.

Mechanical assays do not provide data about the stress applied to bone tissue. In these cases, finite element analysis (FEA) is considered to be ideal to guide clinical research with

biological investigations. Thus, for the construction of the 3D mathematical model, it was necessary to provide data regarding the biological elements corresponding to each part of the maxilla so that force application and the results obtained were as close as possible to the clinical reality [26,27].

For the construction of a lighter 3D model that facilitates the application of intrusive forces, the property of dentin as the only constituent was added to the software since the properties of different dental tissues do not directly affect the results. Thus, clinically observed enamel, dentin, and pulp variations were not considered [10]. The number of elements in the 3D geometrical model is extremely important to increase approximation to the clinical results, providing more reliable models. For example, the hemi-maxilla model using a Y-shaped plate contained 2,831,391 nodes and 1,879,988 elements, necessary to achieve mesh convergence, values higher than those reported in the literature. The model of Holberg (2005) [28] contained 50,000 nodes and 30,000 elements, and the 3D model of the craniofacial complex developed by other studies contained 105,357 nodes and 371,605 elements. [10,28–30]

The finite element analysis performed in this study demonstrated that a larger number of screws together with a better morphology of the miniplate are fundamental to preventing the application of excessive forces to the bone tissue and screw loosening. The morphology of the Y-shaped miniplate with discontinuous screws generates a single plane, as any three non-collinear points determine a unique plane. This configuration possibly confers greater stability to the plate and improves its performance when compared to I- and T-shaped plates.

The strain and compression stress limits of cortical bone are 72–76 MPa and 140–170 MPa, respectively. Thus, regardless of the tests performed, none of the miniplates generated damaging force to bone tissue since the values obtained were extremely low compared to the maximum values. All values obtained were also much lower than the elastic limit of bone, which is 60 MPa [29]. As well as, the miniplates were found to be efficient in withstanding orthodontic forces. The greatest bone stress was generated in the region of the screws but was within physiological limits. The more prone-to-fail configuration seems to be the T-shaped miniplate since it presents a higher stress concentration in the bone tissue. [29,30]

Another study used three 3D models of bone blocks in which I-, Y-, T-, and L-shaped miniplates were installed and forces of 2, 4, and 6 N were applied. The loadings used in the present study are in agreement with other research that investigates miniplate designs for skeletal anchorage and still present values capable of intruding molars as highlighted in experimental studies with animals [23,30]. Furthermore, the distribution of stresses at the root apex, in situations where loading of intrusion forces is performed, can result mainly in apical root resorption or undesirable movements in the bone structure and surrounding tissues. In this sense, the methodology of skeletal anchorage through the use of a miniplate presents better results, since the study showed better performance, that is, less bone stress, for Y and T plates [31]. According to the authors, this finding was due to the greater number of screws in these plate morphologies [23]. This result is contrary to the findings of the present study in which the T-shaped plate exhibited the worst performance in all analyses. One possible explanation for this divergence would be the 3D model used. The use of a model that is faithful to the clinical anatomy allows us to more reliably simulate the changes made in the morphology of the plate when it is modeled to the anatomy of the alveolar zygomatic crest. Such alterations generate changes in the force direction and the behavior of the anchorage device. In the present study, the miniplates followed the maxilla anatomy and warped in the cortical bone surface as occurs in the clinical procedure. Thus, the force was not applied in a perfect straight miniplate, but in a bent geometry that can cause different directional resultants of stress and strain. This step was defined in the modeling process and should be considered in further studies to reproduce the clinical shape of the miniplates in function and not the brand-new miniplates.

The von Mises stress represents the location of the points with the highest stress for ductile solids on the miniplates themselves. In the present study, von Mises stresses were more marked in the most inferior screw, along the long axis of each miniplate, and at the point where the force of the elastic was applied at 2, 4, and 6 N, in agreement with the results of a previous study [30]. The maximum principal stress and von Mises stress values obtained by maximum force applied to the I- and T-shaped miniplates also corroborate the findings of another study employing the same type of movement, which reported a von Mises stress value of 1.66 MPa and maximum principal stress of 39.46 MPa [32].

The lack of randomized controlled clinical trials and the small number of systematic reviews on the subject does not allow us to state that anchorage devices are more effective than conventional orthodontic treatment combined or not with orthognathic surgery [29–36]. In addition, the long-term stability of the outcomes is still a matter of concern, although some studies have demonstrated the stability of the skeletal and soft tissue alterations after 4 years and that most recurrences occur, in a small magnitude, in the first year after treatment [33,37–39].

## 5. Conclusions

Based on the findings of this *in silico* study, the following conclusions were drawn:

1. Within the methodological limitations of the present study, orthodontic miniplates for the treatment of AOB appear to be an effective, safe, and less invasive alternative;
2. After the individualization following the maxilla surface anatomy, the Y-plate showed the best performance since its application generated less stress in bone tissue and its shape was associated with less displacement;
3. Different simulations featuring various cortical bone thicknesses and different implant geometries are needed to better understand the biomechanics of each type of miniplate.

**Author Contributions:** Conceptualization: A.P.M.I., J.D.M.d.M., P.Y.N., D.A.Q., A.L.S.B. and R.D.N.; methodology, A.P.M.I., J.D.M.d.M., P.Y.N., D.A.Q., A.L.S.B. and R.D.N.; formal analysis, A.P.M.I., J.D.M.d.M., P.Y.N., D.A.Q., A.L.S.B., R.D.N. and G.d.R.S.L.; investigation, A.P.M.I., J.D.M.d.M., P.Y.N., D.A.Q., A.L.S.B. and R.D.N.; resources, A.P.M.I., J.D.M.d.M., P.Y.N., D.A.Q., A.L.S.B., R.D.N. and G.d.R.S.L.; data curation, A.P.M.I., J.D.M.d.M., P.Y.N., D.A.Q., A.L.S.B., R.D.N. and G.d.R.S.L.; writing—A.P.M.I., J.D.M.d.M., P.Y.N., D.A.Q., A.L.S.B., R.D.N. and G.d.R.S.L.; A.P.M.I., J.D.M.d.M., P.Y.N., D.A.Q., A.L.S.B. and R.D.N.; supervision, A.L.S.B. and R.D.N.; project administration, A.L.S.B. and R.D.N.; funding acquisition, J.D.M.d.M. All authors have read and agreed to the published version of the manuscript.

**Funding:** This research was funded by the São Paulo Research Foundation (FAPESP—grant numbers 2018/04454-0, 2019/24903-6 and 2021/11499-2).

**Institutional Review Board Statement:** Not applicable.

**Informed Consent Statement:** Not applicable.

**Data Availability Statement:** Data are available upon request.

**Acknowledgments:** Not applicable.

**Conflicts of Interest:** The authors declare no conflict of interest.

## References

1. Almeida, R.R.; Pedrin, R.R.A.; Almeida, M.R.; Ferreira, F.P.C.; Pinzan, A. Displasias vesrticais: Mordida aberta anterior- Tratamento e estabilidade. *R Dent. Press Ortodon. Ortop Facial*. **2003**, *8*, 91–119.
2. Leung, M.T.; Lee, T.C.; Rabie, A.B.; Wong, R.W. Use of miniscrews and miniplates in orthodontics. *J. Oral. Maxillofac Surg*. **2008**, *66*, 1461–1466. [[CrossRef](#)]
3. Sakima, M.T.; Mendonça, A.A.; Ocanha-Júnior, J.M.; Sakima, T. Sistema de Apoio Ósseo para Mecânica Ortodôntica (SAO®)—miniplacas para ancoragem ortodôntica. Parte I: Tratamento da mordida aberta. *Rev. Dent. Press*. **2009**, *14*, 103–116. [[CrossRef](#)]

4. Largura, L.Z.; Argenta, M.A.; Sakima, M.T.; Camargo, E.S.; Guariza-Filho, O.; Tanaka, O.M. Bone stress and strain after use of a miniplate for molar protraction and uprighting: A 3-dimensional finite element analysis. *Am. J. Orthod. Dentofac. Orthop.* **2014**, *146*, 198–206. [[CrossRef](#)]
5. Farret, M.M.; Farret, M.M.; Farret, A.M. Orthodontic camouflage of skeletal Class III malocclusion with miniplate: A case report. *Dent. Press J. Orthod.* **2016**, *21*, 89–98. [[CrossRef](#)]
6. Umemori, M.; Sugawara, J.; Mitani, H.; Nagasaka, H.; Kawamura, H. Skeletal anchorage system for open-bite correction. *Am. J. Orthod. Dentofac. Orthop.* **1999**, *115*, 166–174. [[CrossRef](#)]
7. Lee, H.; Ting, K.; Nelson, M.; Sun, N.; Sung, S.J. Maxillary expansion in customized finite element method models. *Am. J. Orthod. Dentofac. Orthop.* **2009**, *136*, 367–374. [[CrossRef](#)]
8. Faber, J.; Morum, T.F.A.; Leal, S.; Berto, P.M.; Carvalho, C.K.S. Miniplacas permitem tratamento eficiente e eficaz da mordida aberta anterior. *R Dent. Press Ortodon. Ortop Facial.* **2008**, *1*, 144–157. [[CrossRef](#)]
9. Lotti, R.S.; Machado, A.W.; Mazzeiro, E.T.; Landre-Júnior, J. Aplicabilidade científica do método dos elementos finitos. *R Dent. Press Ortodon. Ortop Facial.* **2006**, *11*, 35–43. [[CrossRef](#)]
10. Lee, H.; Nguyen, A.; Hong, C.; Hoang, P.; Pham, J.; Ting, K. Biomechanical effects of maxillary expansion on a patient with cleft palate: A finite element analysis. *Am. J. Orthod Dentofacial Orthop.* **2016**, *150*, 313–323. [[CrossRef](#)]
11. Dal Piva, A.M.O.; Tribst, J.P.M.; Souza, R.O.A.E.; Borges, A.L.S. Influence of Alveolar Bone Loss and Cement Layer Thickness on the Biomechanical Behavior of Endodontically Treated Maxillary Incisors: A 3-dimensional Finite Element Analysis. *J. Endod.* **2017**, *43*, 791–795. [[CrossRef](#)]
12. Möhlhenrich, S.C.; Jäger, F.; Jäger, A.; Schumacher, P.; Wolf, M.; Fritz, U.; Bourauel, C. Biomechanical properties of CAD/CAM-individualized nickel-titanium lingual retainers: An in vitro study. *J. Orofac. Orthop.* **2018**, *79*, 309–319. [[CrossRef](#)]
13. Conci, R.A.; Tomazi, F.H.; Noritomi, P.Y.; Da Silva, J.V.; Fritscher, G.G.; Heitz, C. Comparison of Neck Screw and Conventional Fixation Techniques in Mandibular Condyle Fractures Using 3-Dimensional Finite Element Analysis. *J. Oral. Maxillofac Surg.* **2015**, *73*, 1321–1327. [[CrossRef](#)]
14. Geramy, A.; Bouserhal, J.; Martin, D.; Baghaeian, P. Bone stress and strain modification in diastema closure: 3D analysis using finite element method. *Int. Orthod.* **2015**, *13*, 274–286. [[CrossRef](#)]
15. Matos, J.D.M.; Santos, A.C.M.; Nakano, L.J.N.; De Vasconcelos, J.E.L.; Andrade, V.C.; Nishioka, R.S.; Bottino, M.A.; Lopes, G.R.S. Metal alloys in dentistry: An outdated material or required for oral rehabilitation? *Int. J. Odontostomat.* **2021**, *15*, 702–711. [[CrossRef](#)]
16. Osman, R.B.; Elkhadem, A.H.; Ma, S.; Swain, M.V. Titanium versus zirconia implants supporting maxillary overdentures: Three-dimensional finite element analysis. *Int. J. Oral Maxillofac. Implants.* **2013**, *28*, e198–e208. [[CrossRef](#)]
17. Geng, J.P.; Tan, K.B.; Liu, G.R. Application of finite element analysis in implant dentistry: A review of the literature. *J. Prosthet Dent.* **2001**, *85*, 585–598. [[CrossRef](#)]
18. Kumar, G.P.; Cui, F.; Phang, H.Q.; Su, B.; Leo, H.L.; Hon, J.K. Design considerations and quantitative assessment for the development of percutaneous mitral valve stent. *Med. Eng. Phys.* **2014**, *36*, 882–888. [[CrossRef](#)]
19. Mo, S.S.; Noh, M.K.; Kim, S.H.; Chung, K.R.; Nelson, G. Finite element study of controlling factors of anterior intrusion and torque during Temporary Skeletal Anchorage Device (TSAD) dependent en masse retraction without posterior appliances: Biocreative hybrid retractor (CH-retractor). *Angle Orthod.* **2020**, *90*, 255–262. [[CrossRef](#)]
20. Madfa, A.A.; Kadir, M.R.; Kashani, J.; Saidin, S.; Sulaiman, E.; Marhazlinda, J.; Rahbari, R.; Abdullah, B.J.; Abdullah, H.; Abu Kasim, N.H. Stress distributions in maxillary central incisors restored with various types of post materials and designs. *Med. Eng. Phys.* **2014**, *36*, 962–967. [[CrossRef](#)]
21. De Andrade, G.S.; Tribst, J.P.M.; Dal Piva, A.M.d.O.; Bottino, M.A.; Borges, A.L.S.; Valandro, L.F.; Özcan, M. A study on stress distribution to cement layer and root dentin for post and cores made of CAD/CAM materials with different elasticity modulus in the absence of ferrule. *J. Clin. Exp. Dent.* **2019**, *11*, e1–e8. [[CrossRef](#)]
22. Ramos, A.L.; Zange, S.E.; Terada, H.H.; Hoshina, F.T. Anchorage miniplates in the treatment of anterior open bite. *Rev Dent Press Ortodon. Ortop. Facial.* **2008**, *13*, 134–143. [[CrossRef](#)]
23. Huang, Y.W.; Chang, C.H.; Wong, T.Y.; Liu, J.K. Bone stress when miniplates are used for orthodontic anchorage: Finite element analysis. *Am. J. Orthod. Dentofac. Orthop.* **2012**, *142*, 466–472. [[CrossRef](#)]
24. Greenlee, G.M.; Huang, G.J.; Chen, S.S.; Chen, J.; Koepsell, T.; Hujuel, P. Stability of treatment for anterior open-bite malocclusion: A meta-analysis. *Am. J. Orthod. Dentofac. Orthop.* **2011**, *139*, 154–169. [[CrossRef](#)]
25. Park, Y.C.; Lee, H.A.; Choi, N.C.; Kim, D.H. Open bite correction by intrusion of posterior teeth with miniscrews. *Angle Orthod.* **2008**, *78*, 699–710. [[CrossRef](#)]
26. Alves, A.; Cacho, A.; San Roman, F.; Gerós, H.; Afonso, A. Mini implants osseointegration, molar intrusion and root resorption in Sinclair minipigs. *Int. Orthod.* **2019**, *17*, 733–743. [[CrossRef](#)]
27. Kitamura, E.; Stegaroiu, R.; Nomura, S. Biomechanical aspects of marginal bone resorption around osseointegrated implants: Considerations based on a three-dimensional finite element analysis. *Clin. Oral. Implant. Res.* **2004**, *15*, 401–412. [[CrossRef](#)]
28. Holberg, C.; Steinhäuser, S.; Geis, P.; Rudzki-Janson, I. Cone-beam computed tomography in orthodontics: Benefits and limitations. *J. Orofac. Orthop.* **2005**, *66*, 434–444. [[CrossRef](#)]
29. Trabelsi, N.; Yosibash, Z.; Wutte, C.; Augat, P.; Eberle, S. Patient-specific finite element analysis of the human femur—A double-blinded biomechanical validation. *J. Biomechanics.* **2011**, *44*, 1666–1672. [[CrossRef](#)]

30. Papavasiliou, G.; Kamposiora, P.; Bayne, S.C.; Felton, D.A. Three-dimensional finite element analysis of stress-distribution around single tooth implants as a function of bony support, prosthesis type, and loading during function. *J. Prosthet Dent.* **1996**, *76*, 633–640. [[CrossRef](#)]
31. Daimaruya, T.; Nagasaka, H.; Umemori, M.; Sugawara, J.; Mitani, H. The influences of molar intrusion on the inferior alveolar neurovascular bundle and root using the skeletal anchorage system in dogs. *Angle Orthod.* **2001**, *71*, 60–70. [[PubMed](#)]
32. Çifter, M.; Saraç, M. Maxillary posterior intrusion mechanics with mini-implant anchorage evaluated with the finite element method. *Am. J. Orthod. Dentofac. Orthop.* **2011**, *140*, e233–e241. [[CrossRef](#)]
33. Nalbantgil, D.; Tozlu, M.; Ozdemir, F.; Oztoprak, M.O.; Arun, T. FEM analysis of a new miniplate: Stress distribution on the plate, screws and the bone. *Eur. J. Dent.* **2012**, *6*, 9–15. [[CrossRef](#)] [[PubMed](#)]
34. Veziroglu, F.; Uckan, S.; Ozden, U.A.; Arman, A. Stability of zygomatic plate-screw orthodontic anchorage system: A finite element analysis. *Angle Orthod.* **2008**, *78*, 902–907. [[CrossRef](#)] [[PubMed](#)]
35. Iwasa, A.; Horiuchi, S.; Kinouchi, N.; Izawa, T.; Hiasa, M.; Kawai, N.; Yasue, A.; Hassan, A.H.; Tanaka, E. Skeletal anchorage for intrusion of bimaxillary molars in a patient with skeletal open bite and temporomandibular disorders. *J. Orthod Sci.* **2017**, *6*, 152–158.
36. Assis, D.S.; Xavier, T.A.; Noritomi, P.Y.; Gonçalves, E.S. Finite element analysis of bone stress after SARPE. *J. Oral. Maxillofac Surg.* **2014**, *72*, 167.e1–167.e7. [[CrossRef](#)]
37. Matos, J.D.M.; Nakano, L.J.N.; Bottino, M.A.; Jesus, R.H.; Maciel, L.C. Current considerations for dental ceramics and their respective union systems. *Rev. Bras. Odontol.* **2020**, *77*, 1768. [[CrossRef](#)]
38. Matos, J.D.M.; Lopes, G.D.R.S.; Nakano, L.J.N.; Ramos, N.C.; Vasconcelos, J.E.L.; Bottino, M.A.; Tribst, J.P.M. Biomechanical evaluation of 3-unit fixed partial dentures on monotype and two-piece zirconia dental implants. *Comput. Methods Biomech. Biomed. Engin.* **2022**, *25*, 239–246. [[CrossRef](#)]
39. Matos, J.D.M.d.; Lopes, G.d.R.S.; Queiroz, D.A.; Pereira, A.L.J.; Sinhoretí, M.A.C.; Ramos, N.C.; Lino, V.; Oliveira, F.R.; Borges, A.L.S.; Bottino, M.A. Influence of the Peek Abutments on Mechanical Behavior of the Internal Connections Single Implant. *Materials* **2022**, *15*, 8133. [[CrossRef](#)]